Human-induced loading and dynamic response of footbridges in the vertical direction due to restricted pedestrian traffic

HUMAN-INDUCED LOADING AND DYNAMIC RESPONSE OF FOOTBRIDGES IN THE VERTICAL DIRECTION DUE TO RESTRICTED PEDESTRIAN TRAFFIC

Fiammetta Venuti[1], **Federica Tubino**[2]

[1] Politecnico di Torino
Viale Mattioli, 39, 10125 Torino, Italy
e-mail: fiammetta.venuti@polito.it

[2] Università di Genova
Via Montallegro, 1, 16145 Genova, Italy
e-mail: federica.tubino@unige.it

ABSTRACT

Despite extensive research in the field of human-induced vibration in the last twenty years, there is still lack of reliable load and response models to assess vibration serviceability of footbridges under human-induced excitation, especially with reference to crowded conditions. This paper aims to provide a reliable characterization of pedestrian-induced loading on footbridges in restricted traffic condition, and to compare the reliability of current guidelines and advanced spectral models in the serviceability assessment of footbridges with respect to vertical vibrations. Numerical simulations of restricted pedestrian traffic are carried out through an agent-based model, considering variable pedestrian densities and deck widths. The probability distribution of the step frequency and the power spectral density function of the modal force are obtained numerically. Based on the numerical results, a Modified Generalized Equivalent Spectral Model is proposed. Finally, two numerical examples are analyzed to assess the reliability of current guidelines and of the Modified Generalized Equivalent Spectral Model in the estimate of the maximum footbridge acceleration.

Keywords: Crowd Modelling, Footbridges, Pedestrian Loading, Restricted Traffic, Serviceability Assessment, Spectral Model, Vertical Vibrations.

1 INTRODUCTION

Vibration serviceability assessment of footbridges under human-induced excitation requires the availability of suitable load models. In the last twenty years, extensive research has been carried out to provide a reliable characterization of walking excitation, focusing on three key factors, namely the variability of parameters influencing pedestrian-induced dynamic load, the interaction among pedestrians and human-structure interaction.

The variability of loading parameters is usually classified into in the so-called *intra-subject* (Zivanovic et al., 2007, Racic & Brownjohn, 2011, Sahnaci & Kasperski, 2011) and *inter-subject variability* (Sahnaci & Kasperski, 2005, Caprani et al., 2012, Dang and Zivanovic, 2015). Intra-subject variability is the intrinsic variability of the loading exerted by a single pedestrian along its trajectory and is due to the variation of load amplitude and timing (and hence of step frequency) between successive steps of the same individual. Inter-subject variability refers to the variability of loading parameters among different individuals. Specifically, the parameters that could vary among different pedestrians are step frequency, magnitude of the dynamic component of the force, pedestrian weight and walking velocity. Van Nimmen et al. (2017) have shown that, in multi-pedestrian loading, the impact of inter-subject variability on the structural dynamic response prevails over that of intra-subject variability.

The interaction among pedestrians occurs for high pedestrian density. Experimental tests (Butz et al., 2008, Araujo et al., 2009, Pimentel et al., 2013) have shown that pedestrian interaction mainly results in a decrease of mean and standard deviation values of walking velocity and step frequency as the crowd density increases.

Human-structure interaction can occur both in the lateral and vertical directions (for a literature review, see, e.g., Shahabpoor et al., 2016, Fujino and Siringoringo 2016). In the case of vertical vibrations, which is the specific focus of the present study, the effect of human-structure interaction can be approximately taken into account suitably modifying the footbridge dynamic properties by adding mass and damping (He & Xie, 2018).

Serviceability assessment of footbridges could be carried out through time-domain or frequency domain (or spectral) approach (Zivanovic et al., 2005).

Within time-domain approach, inter- and intra-subject variability can be taken into account by adopting probabilistic time-domain force-models, i.e., by describing each loading parameter as a random variable characterized by its probability distribution. The structural response is then characterized probabilistically through a Monte Carlo approach (e.g., Zivanovic et al., 2010, Racic & Brownjohn, 2011, Tubino & Piccardo, 2016), starting from a set of samples of the loading time histories obtained by sampling the load parameters from their probability distributions. In this framework, the interaction among pedestrians can be included in numerical simulations through the adoption of microscopic crowd models (e.g., Helbing & Molnar, 1995), describing the motion of each pedestrian, whose velocity is determined by the interactions with the environment and the surrounding pedestrians (Carroll et al., 2012, Venuti et al., 2016, Gao et al., 2017). In addition, human-structure interaction in the vertical direction can be included by modelling pedestrians as moving single-degree of freedom systems with deterministic or random properties (see, e.g., Caprani & Ahmadi, 2016, Venuti et al., 2016, Van Nimmen et al., 2017, Tubino, 2018) or through the inverted pendulum model (Macdonald 2009).

The time-domain approach, relying on Monte Carlo simulations, allows to suitably account for all the stochastic factors affecting footbridges' serviceability assessment; however, it may be time-consuming and not practical at the design stage. As an alternative, the most recent design guidelines for the serviceability assessment of footbridges (SETRA, 2006, Feldmann, 2008) propose simplified procedures to determine the peak response based on a deterministic equivalent uniformly-distributed resonant load that should produce the same maximum

dynamic response induced by random pedestrians. For sparse traffic, the amplitude of the equivalent uniformly-distributed load has been obtained from Monte Carlo simulations modelling the single-pedestrian loading as a moving harmonic and taking into account inter-subject variability by assuming a normal distribution of the step frequencies with a mean value coincident with the footbridge natural frequency. For dense traffic, interaction among pedestrians is approximately considered by assuming all pedestrians walking in step. Despite this procedure is very simple to apply and specifically conceived for design, some of the key factors influencing the pedestrian load, such as the dependence of step frequency on pedestrian density and the human-structure interaction, are not adequately taken into account. Moreover, the load is applied in resonance with the structure in a worst-case perspective, often leading to significant overestimation of the structural response.

Spectral approach has received increasing attention in the last decade since it allows considering the inherent randomness of walking parameters (inter-subject variability) avoiding time consuming numerical simulations. Pedestrian loading is modelled as an equivalent stationary random process defined by a power spectral density function and a coherence function (e.g., Brownjohn et al., 2004, Piccardo & Tubino, 2012, Tubino & Piccardo, 2016). Based on this loading model, simple expressions for the evaluation of the maximum footbridge dynamic response have been introduced (e.g., Piccardo & Tubino, 2012, Van Nimmen et al., 2020). Most spectral models in the literature refer to unrestricted traffic conditions, with the exception of the Generalized Equivalent Spectral Model (GESM) introduced by Ferrarotti and Tubino (2016). In the GESM, the interaction among pedestrians is considered in two ways: (1) the mean step frequency of pedestrians is expressed as a function of the crowd density; (2) a coherence function is introduced to model the increasing correlation of the loading at different locations for increasing crowd density, when pedestrians tend to synchronize their step frequency with the neighboring ones. Due to the lack of experimental data, the coherence function has been defined in a qualitative physically-based way. Therefore, a numerical and/or experimental validation of the model is still needed before it could be confidently applied. A procedure to approximately account for human-structure interaction in the vertical direction within the spectral approach has been proposed by Bassoli et al. (2018).

Based on the above review of the available procedures for vibration serviceability assessment, the spectral approach is considered to have great potential to be easily applied in the design stage and to provide accurate results as long as a reliable equivalent spectral model of the loading is available. Thus, a numerical and/or experimental validation of the GESM reliability in predicting the harmonic content of the loading exerted by pedestrians in restricted traffic condition and the resulting footbridge dynamic response is required.

The aim of the proposed work is to provide a reliable probabilistic characterization of human-induced loading and of footbridges' dynamic response taking into account inter-, intra-subject variability and the interaction among pedestrians and to evaluate the reliability of simplified methods proposed by guidelines and of the GESM in the assessment of footbridges' vibration serviceability in crowded conditions. The study focuses on vertical excitation and, at this stage, neglects human-structure interaction.

Due to the lack of experimental measurements in dense traffic conditions, numerical crowd dynamics simulations are carried out for increasing values of pedestrian density relying on a microscopic agent-based model of pedestrian dynamics. For each traffic condition, a set of numerical simulations is carried out through a Monte Carlo approach, allowing to obtain a probabilistic characterization of pedestrian step frequencies, and to perform serviceability analysis in the time domain. More in detail, the simulations are performed on three ideal footbridges with three different widths, crossed by unidirectional flow of pedestrians with densities varying in the range 0.3-1.5 ped/m^2. The trajectories and velocities of each pedestrian

are obtained; then, instantaneous pedestrian step frequencies are estimated through a velocity-density law from the literature. At a second step, pedestrians are schematized as moving loads with time-variant step frequency, because of the variation of walking velocity during each pedestrian crossing induced by interactions among pedestrians. Then, the force exerted on the footbridge by the crowd is obtained and the dynamic response of two footbridges, considered as case studies, is estimated numerically. For each value of footbridge width and pedestrian density, the probability distribution of the pedestrian step frequency and the power spectral density function (psdf) of the modal force are derived. The effect of variation of the footbridge width and of the pedestrian density on such quantities is analyzed. Furthermore, the numerically-estimated psdf of the modal force is compared with the analytical expression provided by the GESM. A critical analysis is provided, and a Modified GESM is proposed in order to fit numerical results. Finally, the mean value of the maximum dynamic response of the two case studies is compared with the predictions provided by current design guidelines and by the Modified GESM.

The outline of the paper is as follows. In Section 2, the analytical formulation is provided, including time-domain formulation (Section 2.1), spectral approach (Section 2.2) and Guidelines procedures (Section 2.2). Section 3 reports the results of crowd dynamics simulations (Section 3.1), with focus on the probability distribution of step frequencies (Section 3.2) and on the spectral properties of pedestrian-induced modal loading (Section 3.3). Finally, Section 4 provides a numerical application to two footbridges. The conclusions and some prospects of this research are formulated in Section 5.

2 ANALYTICAL FORMULATION

Let us consider a footbridge, modelled as a linear mono-dimensional classically damped dynamical system. Its equation of motion can be written as follows:

$$m_s(x)\frac{\partial^2 q(x,t)}{\partial^2 t}+\mathcal{C}\left[\frac{\partial q(x,t)}{\partial t}\right]+\mathcal{L}\left[q(x,t)\right]=f(x,t) \tag{1}$$

where q is the vertical displacement of the footbridge, x is the abscissa along the structure longitudinal axis, t is the time, $m_s(x)$ is the structural mass, $\mathcal{C}$ is the damping operator, $\mathcal{L}$ is the stiffness operator, $f(x,t)$ is the external force.

Under the hypothesis of classical damping, Equation (1) is usually solved applying the principal transformation. Considering the contribution of one vibration mode (namely the j-th), the structural displacement can be expressed as:

$$q(x,t)=\varphi_j(x)\,p_j(t) \tag{2}$$

where $\varphi_j(x)$ is the j-th mode of vibration and $p_j(t)$ is the corresponding principal coordinate.

The equation of motion of the j-th principal coordinate is expressed as:

$$\ddot{p}_j(t)+2\xi_j\omega_j\dot{p}_j(t)+\omega_j^2 p_j(t)=\frac{1}{M_j}F_j(t) \tag{3}$$

being ξ_j, ω_j and M_j the j-th modal damping ratio, natural circular frequency and modal mass, respectively; $F_j(t)$ is the j-th modal force:

$$F_j(t)=\int_0^L f(x,t)\varphi_j(x)\,\mathrm{d}x \tag{4}$$

being L the length of the structure.

In this Section, three approaches are described for assessing pedestrian-induced response of footbridges: time-domain approach (Section 2.1), spectral approach (Section 2.2) and simplified procedures provided by current guidelines (Section 2.3).

2.1 Time-domain approach

When dealing with human-induced vibrations of footbridges, pedestrians are commonly schematized as moving loads (Zivanovic et al., 2005). The force per unit length exerted by N_p pedestrians is expressed as the sum of the forces exerted by each single pedestrian as follows:

$$f(x,t) = \sum_{i=1}^{N_p} f_i(t)\delta\left[x - x_i(t)\right] \tag{5}$$

where $x_i(t)$ and $f_i(t)$ are the instantaneous position and the force exerted by the i-th pedestrian, respectively, and $\delta(\bullet)$ is the Dirac delta function.

Van Nimmen et al. (2017) showed that the effect of inter-subject variability on the structural dynamic response prevails over that of intra-subject variability. Thus, the force $f_i(t)$ can be schematized as a periodic function. Focusing attention on the first walking harmonic and neglecting the interaction among pedestrians (i.e., considering unrestricted pedestrian traffic), the force is modelled as a harmonic function with fixed frequency (Zivanovic et al., 2005).

When the interaction among pedestrians is taken into account, then the step frequency of each pedestrian is influenced by the presence of surrounding pedestrians. If the interaction is modelled numerically, e.g., with microscopic crowd dynamics models (e.g., Helbing & Molnar, 1995, Venuti et al., 2016), the instantaneous position x_i and velocity v_i of the i-th pedestrian are the output of the simulation. The literature provides relationships between the step frequency n_i and the step velocity v_i (e.g., Butz et al., 2008, Bruno & Venuti, 2009), allowing to derive the instantaneous step frequency from the instantaneous pedestrian velocity. Since the pedestrian step frequency $n_i(t)$ is time variant during footbridge crossing, the force exerted by the i-th pedestrian can be modelled as a sinusoidal carrier signal, with a modulated base frequency $n_{m,i}$, as follows (Lathi, 1998):

$$f_i(t) = \alpha_i G_i \sin\left[2\pi n_{m,i} t + 2\pi \int_0^t \left(n_i(\tau) - n_{m,i}\right) \mathrm{d}\tau\right] \tag{6}$$

where $n_{m,i}$ is the mean value of the instantaneous step frequency during footbridge crossing time T_i. Furthermore, α_i and G_i are the dynamic load factor (DLF) and the weight of the i-th pedestrian, respectively.

The time-domain expression of the modal load is obtained substituting Equation (5) into Equation (4), and it is given by:

$$F_j(t) = \sum_{i=1}^{N_p} f_i(t)\varphi_j\left[x_i(t)\right] \tag{7}$$

The principal coordinate is then obtained solving Equation (3), taking into account Equation (7) with $f_i(t)$ given by Equation (6). In order to characterize probabilistically the dynamic response, a suitable number of numerical simulations have to be performed through Monte Carlo approach by sampling the load parameters from their probability distributions and a statistical analysis of results in terms of standard deviation and/or maximum value of the footbridge acceleration has to be carried out.

2.2 Spectral Approach

The spectral approach is based on the definition of the cross-power spectral density function (cpsdf) of the force per-unit-length $S_{ff}(x,x',n)$, which, under the assumption of uniform equivalent loading, is given by:

$$S_{ff}\left(x,x';n\right)=S_{f}\left(n\right)Coh_{ff}\left(x,x';n\right) \tag{8}$$

where $S_f(n)$ is the psdf of the force per-unit-length, and $Coh_{ff}(x,x',n)$ is its coherence function.

According to the GESM proposed by Ferrarotti and Tubino (2016), the psdf of the pedestrian-induced force-per-unit-length is given by:

$$S_{f}\left(n\right)=\frac{\left(\alpha_{m}G_{m}\right)^{2}}{\varepsilon L}\frac{N_{p}}{4}p_{N}\left(n\right) \tag{9}$$

where α_m and G_m are the mean value of the DLF and of pedestrian weight, respectively, ε is interpreted as the separation distance that each pedestrian interposes with others to avoid contact, assumed as $\varepsilon = 4$ m, $p_N(n)$ is the probability density function (pdf) of the step frequency n. In the GESM, a Gaussian distribution is assumed for the step frequency, with a fixed standard deviation n_{std} = 0.18 Hz and a mean value n_m expressed as a function of the mean walking velocity v_m (Bruno & Venuti, 2009):

$$n_{m}=0.35v_{m}^{3}-1.59v_{m}^{2}+2.93v_{m} \tag{10}$$

being the mean walking velocity v_m related to pedestrian density ρ through the fundamental law:

$$v_{m}\left(\rho\right)=v_{\max}\left\{1-\exp\left[-\gamma\rho_{\max}\left(\frac{1}{\rho}-\frac{1}{\rho_{\max}}\right)\right]\right\} \tag{11}$$

with ρ_{max} = 5.4 ped/m^2, γ = 0.354, v_{max} = 1.34 m/s.
The coherence function is expressed as follows:

$$Coh_{ff}\left(x,x';n\right)=\begin{cases}1 & \text{if} \quad \left|x-x'\right|<\varepsilon\\ \exp\left[-C\left(\left|x-x'\right|-\varepsilon\right)\right] & \text{otherwise}\end{cases} \tag{12}$$

being the exponential decay coefficient C a function of the mean step frequency n_m, $C = \exp(C_1 n_m + C_2)$, (C_1 = 22.7, C_2 = -41).

The psdf of the modal force for a generic mode shape $\varphi_j(x)$ is given by (Ferrarotti & Tubino, 2016):

$$S_{F_j}\left(n\right)=S_{f}\left(n\right)\chi_{j}\left(n\right) \tag{13}$$

where $\chi_j(n)$ is the admittance function, defined as follows:

$$\chi_{j}\left(n\right)=\int_{0}^{L}\int_{0}^{L}Coh_{ff}\left(x,x';n\right)\varphi_{j}\left(x\right)\varphi_{j}\left(x'\right)dxdx' \tag{14}$$

Under the assumption of unrestricted traffic, and considering the first mode shape of a simply-supported beam $\varphi_j(x)=\sin(\pi x/L)$, the psdf of the modal force is given by (Piccardo & Tubino, 2012, Ferrarotti & Tubino, 2016):

$$S_{F_j\mathrm{unr}}(n) = (\alpha_m G_m)^2 \frac{N_p}{4} p_N(n) \tag{15}$$

The psdf of the acceleration of the *j*-th principal coordinate is given by:

$$S_{\ddot{p}_j}(\omega) = \omega^4 \left|H_j(\omega)\right|^2 S_{F_j}(\omega) \tag{16}$$

where $H_j(\omega)$ is the frequency response function of the *j*-th principal coordinate:

$$H_j(\omega) = \frac{1}{M_j} \frac{1}{\omega_j^2 - \omega^2 + 2\mathrm{i}\xi_j \omega_j \omega} \quad . \tag{17}$$

Furthermore, $S_{F_j}(\omega)$ is the single-sided psdf of the modal load:

$$S_{F_j}(\omega) = \frac{S_{F_j}(n)}{2\pi} \tag{18}$$

The variance of the acceleration of the *j*-th principal coordinate can be obtained as follows:

$$\sigma_{\ddot{p}_j}^2 = \int_0^{+\infty} S_{\ddot{p}_j}(\omega)\mathrm{d}\omega = \int_0^{+\infty} \omega^4 \left|H_j(\omega)\right|^2 S_{F_j}(\omega)\mathrm{d}\omega \tag{19}$$

Approximate closed-form solutions have been introduced for evaluating the integral in Equation (19), providing reliable estimates when the harmonic content of the loading is concentrated around the structural natural frequency (Piccardo & Tubino, 2012), and when the mean step frequency is far from the natural frequency of the structure (Van Nimmen et al., 2020), respectively.

According to Davenport's formulation (Davenport, 1964), the expected value of the maximum acceleration is given by:

$$\ddot{q}_{\max} = \mathrm{E}\left[\ddot{p}_{J_{\max}}\right] = g_{\ddot{p}_j} \sigma_{\ddot{p}_j} \tag{20}$$

being the peak factor $g_{\ddot{p}_j}$ defined as:

$$g_{\ddot{p}_j} = \sqrt{2\ln(2\nu_{\ddot{p}_j} T)} + \frac{0.5772}{\sqrt{2\ln(2\nu_{\ddot{p}_j} T)}} \qquad T = \frac{NL}{v_m} \qquad \nu_{\ddot{p}_j} \approx \frac{\omega_j}{2\pi} \qquad N = 10 \tag{21}$$

2.3 Guidelines Procedures

Advanced design guidelines (e.g. SETRA, 2006, Feldmann, 2008) provide simplified procedures to assess vibration serviceability of footbridges. Dealing with vibrations in the vertical direction, SETRA (2006) guideline provides an equivalent uniformly-distributed resonant loading condition. HiVOSS (Feldmann 2008) recommends two alternative methods to calculate the maximum footbridge acceleration, named, respectively, SDOF method, which is almost coincident with the loading model proposed by SETRA and provides results in full accordance with that (Van Nimmen et al., 2014) and response spectra method. In this Section, the two methods proposed by HiVOSS guideline are described.

2.3.1 HiVOSS SDOF method

For footbridges with a natural frequency n_j ($=\omega_j/2\pi$) in the interval [1.25 2.1] Hz, a resonant uniformly distributed harmonic load $f(t)$ (N/m^2) is defined as follows:

$$f(t) = \alpha_m G_m \cos\left(2\pi n_j t\right) N'\psi \qquad \alpha_m G_m = 280 \text{ N}$$

$$N' = \begin{cases} \dfrac{10.8\sqrt{\xi_j N_p}}{S} & \text{if} \quad \rho \le 1 \text{ ped/m}^2 \\ \dfrac{1.85\sqrt{N_p}}{S} & \text{if} \quad \rho > 1 \text{ ped/m}^2 \end{cases}$$

$$\psi = \begin{cases} 0 & n_j < 1.25 \text{ or } n_j > 2.3 \\ \dfrac{\left(n_j - 1.25\right)}{0.45} & 1.25 < n_j < 1.7 \\ 1 & 1.7 < n_j < 2.1 \\ 1 - \dfrac{\left(n_j - 2.1\right)}{0.2} & 2.1 < n_j < 2.3 \end{cases} \tag{22}$$

where S (=BL) is the loaded surface of the deck and N' represents the equivalent number of perfectly synchronized pedestrians per square meter generating the 95th percentile of the peak acceleration response induced by random pedestrians. The load should be applied with the same sign as the one of the considered mode shape. The load model proposed by SETRA (2006) is coincident with Equation (22) except for a slightly different definition of the ψ factor.

Substituting Equation (22) into Equation (4), the maximum footbridge acceleration is then given by:

$$\ddot{q}_{\max_{HE}} = \frac{\alpha_m G_m N' B \int_0^L \varphi_j(x)\,\mathrm{d}x}{2\xi_j M_j} \tag{23}$$

2.3.2 HiVOSS Response spectra method

Analogously to the spectral approach (Equation (20)), the response spectra method allows to estimate the maximum footbridge acceleration as follows:

$$\ddot{q}_{\max_{HS}} = g_{HS}\sigma_{HS} \tag{24}$$

being g_{HS} and σ_{HS} the peak factor and the standard deviation of the acceleration, respectively. Such coefficients depend on the pedestrian density and have been derived numerically from Monte Carlo simulations based on time domain simulations of the dynamic response of different footbridges to variable pedestrian streams, assuming the pedestrian step frequency as a random variable with mean and standard deviation values depending on the stream density. This method approximately takes into account inter-subject variability and the interaction among pedestrians.

The following approximate expression is provided for the standard deviation:

$$\sigma_{HS}^2 = k_1 \xi_j^{k_2} \frac{C_\sigma \sigma_F^2}{M_j^2}$$
$$k_1 = a_1 n_j^2 + a_2 n_j + a_3 \qquad k_2 = b_1 n_j^2 + b_2 n_j + b_3 \qquad \sigma_F^2 = k_F N_p \tag{25}$$

The peak factor in Equation (24) and the coefficients in Equation (25) are listed in Table 1.

ρ [ped/m^2]	k_F	C_σ	a_1	a_2	a_3	b_1	b_2	b_3	g_{HS}
≤ 0.5	1.20×10^{-2}	2.95	-0.07	0.60	0.075	0.003	-0.040	-1.000	3.92
1.0	7.00×10^{-3}	3.70	-0.07	0.56	0.084	0.004	-0.045	-1.000	3.80
1.5	3.34×10^{-3}	5.10	-0.08	0.50	0.085	0.005	-0.060	-1.005	3.74

Table 1: Coefficients for HiVOSS Response Spectra Method (Feldmann, 2008).

3 NUMERICAL SIMULATION OF RESTRICTED PEDESTRIAN TRAFFIC

This Section describes the results of numerical simulations of pedestrian traffic along three ideal footbridges. After an illustration of the numerical simulations (Section 3.1), results are presented in terms of probabilistic characterization of walking velocities and step frequencies (Section 3.2) and spectral properties of pedestrian-induced loading (Section 3.3).

3.1 Crowd dynamics simulations

Crowd dynamics simulations are carried out through the commercial software MassMotion 9.5 by Oasys Ltd (Arup, 2017). MassMotion is a 3D agent-based simulation tool, which has been verified in both normal and evacuation scenarios (Arup, 2020a, 2020b) and validated against experimental data (Rivers et al., 2014). In agent-based models, a system is described as a collection of intelligent, autonomous, decision-making entities known as 'agents' (see Challenger et al., 2009 for a comprehensive review): this is considered as the most realistic way to simulate pedestrian dynamics. Even though MassMotion has been originally conceived to address evacuation events, the data and theories upon which it relies on refer to normal human behaviour (Arup, 2020b): there is, actually, evidence that people in an emergency tend to behave normally and panic is very rare (Challenger at al., 2009). In MassMotion each pedestrian is modelled as an individual agent, with unique personality and physical characteristics, who tries to reach his destination by moving inside the environment at his desired velocity.

The motion of the agents is determined in two steps. In the first step (Navigation) a decision-making process allows the agents to analyse the physical environment and congestion between the actual location and destination to select the most appropriate route. Since pedestrian behaviour is driven by the principle of 'least effort' (Challenger et al., 2009), the route is chosen as the one corresponding to the lowest cost, i.e., the lowest time to reach the destination, among all the possible routes. To do so, at the beginning of the analysis the software automatically creates a network from all the geometric components of the environment. Thus, each agent is able to calculate the cost of all the possible routes to his destination according to the following equation:

$$C_R = \sum W_i T_i \tag{26}$$

where C_R is the route cost, W_i are the weights associated to each cost component and T_i is the i-th cost component in seconds. The cost components that are relevant for the specific set-up analysed in this study are described in Table 2. Moreover, each route choice is assigned a small random factor. As a result, agents will on occasion choose slightly less than optimal routes ensuring that not all agents make the same choice when routes are very close in cost.

Cost component	Description
Downstream horizontal distance	The shortest possible horizontal distance from the intermediate target to the destination
Near horizontal distance	The horizontal distance from the agent to the intermediate target
Queue time	The expected time it will take to queue for the intermediate target

Table 2: Cost components (costs in distance are converted in time by dividing them by agent's velocity).

Once the agent has decided the best route, i.e., his desired direction, in the second step (Movement) the direction and velocity of each agent is determined through a Social Forces algorithm, which implements a modified version of the social force model by Helbing and Molnar (1995). The agents' motion is determined at each time step as the consequence of a set of "social forces" acting on each agent, according to the following coupled equations:

$$\begin{cases} \dot{\mathbf{r}}_i = \mathbf{v}_i \\ \dot{\mathbf{v}}_i = \mathbf{F}_i + \mathbf{F}_i' \end{cases} \tag{27}$$

where $\mathbf{r}_i$ is the agent position at time t, $\mathbf{v}_i$ is the agent velocity, $\mathbf{F}_i$ the force acting on the i-th agent and $\mathbf{F}_i'$ is the fluctuation term taking into account random variations of the pedestrian behaviour.

The social forces describe the motivation of each pedestrian to perform certain actions and, in the original formulation (Helbing & Molnar, 1995), comprise the following components: an acceleration/deceleration term towards the desired velocity of motion (Goal); repulsive terms that model the attempt to avoid collisions with other pedestrians (Neighbour) and with borders or obstacles; an attractive term that describes the attraction of pedestrians towards other people (e.g. familiar people) or objects (e.g. panoramic view) (Cohesion). The force components implemented in MassMotion are described in Table 3: besides the basic forces (Goal, Neighbour, Cohesion), some other terms have been added with respect to the original formulation to improve general pedestrian movement with respect to flow rates, crowd density, collision avoidance, and general queuing. The Social Forces algorithm has been calibrated to obtain the people flows corresponding to the Levels of Service defined by Fruin (1971) (Arup, 2020b).

Force	Description
Goal	Force required to nudge agent so that it is at its desired speed heading towards its target
Neighbour	Repulsive force from each neighbour within range
Cohesion	Force pushing towards centroid of neighbours with similar targets
Collision	Force pushing agent away from collisions with oncoming neighbours
Drift	Force pushing agent in bias direction when faced with oncoming agents in narrow spaces
Orderly Queuing	Force pushing agents towards the middle of a target when approaching

Table 3: Forces acting on agents.

Pedestrians are assigned physical and behavioural attributes through the definition of an Agent Profile. According to the default profile, which has been adopted for the simulations, pedestrians' desired velocities are randomly assigned from a truncated Gaussian distribution, with the following parameters: mean value v_m = 1.35 m/s; standard deviation v_{std} = 0.25 m/s; minimum value v_{min} = 0.65 m/s; maximum value v_{max} = 2.05 m/s (after Fruin, 1971). Moreover, the pedestrian desired velocity is modified as a function of the density in the agent's neighbourhood. Specifically, the relationship between density and velocity is set according to the work of Fruin (1971), which is based on data collected in the New York Subway. This constraint also avoids non-rational speed values in certain environments. In the Agent Profile the user can set other parameters, such as the direction bias, i.e. the cultural preference of keeping right or left when facing opposing flow, and the values of the cost weights W_i (Equation (26)). According to the default profile, the latter are randomly assigned to each pedestrian from uniform distributions in the range 0.75-1.25. The generation of random values of some of the model parameters assures that inter-subject variability is taken into account. Intra-subject variability, i.e., slight variations of each pedestrian walking parameters during walking, is a direct consequence of the interaction among the pedestrians and with the environment.

Numerical simulations are carried out on three ideal footbridges, characterized by the same length L = 60 m, and three different widths: B = 1.5 m, B = 2.7 m, B = 4.5 m. The sampling period is set $T_{s,c}$ = 0.2 s. Pedestrian initial positions are randomly distributed in a "starting area" before the footbridge entrance, ten times longer than the footbridge length: this assures that pedestrians are initially uniformly distributed with a crowd density ρ. Hence, the total number of generated pedestrians is set equal to $10\rho BL$. Four values of crowd density, [0.3 0.7 1.1 1.5] ped/m^2, from unrestricted to extremely dense pedestrian traffic, are considered. For each crowd density, 100 simulations are performed to obtain statistical reliability. Figure 1 plots an example of variation of density in time during a simulation (B = 2.7 m).

For each simulation, mean values of the pedestrian density and velocity are calculated during the period of full occupancy T_{full}. The lower bound of T_{full} is determined as the first time instant when the 95% of the mean number of pedestrians $N_p=\rho BL$ are on the footbridge. The upper bound of T_{full} is obtained as the time at which the average crowd density equals the desired value. The mean pedestrian density and velocity of the single simulations are then averaged over 100 simulations.

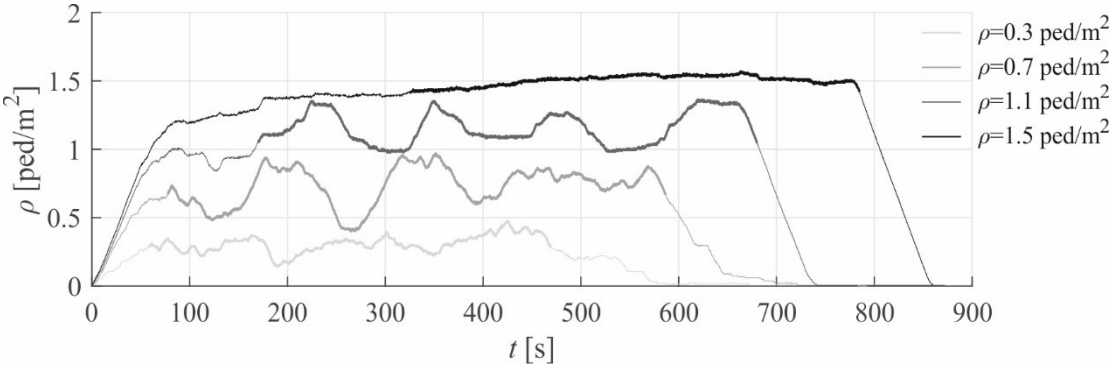

Figure 1: Example of variation of ρ versus time (B=2.7 m). Thicker lines highlight T_{full}.

3.2 Probabilistic characterization of walking velocities and step frequencies

Figure 2 plots the velocity-density relation resulting from crowd simulations (MM) for the three footbridge widths, together with the fundamental law in Equation (11) and other empirical relationships reported in the literature, obtained from experimental measurements in real environments (source Daamen, 2004). It can be observed that the numerical results fall within the range of state-of-the-art relationships, thus proving validation of the software for the considered traffic conditions. It is worth pointing out that the velocity-density relationship is strongly related to the external conditions in which it has been measured. For instance, both Sarkar and Janardhan and Fruin performed observations in transportation terminals, where people usually walk in a hurry, thus obtaining higher velocities with respect to Virkler and Elayadath, who observed people slowly moving after a football match. Moreover, all the reported experimental data have been measured in wide spaces, where higher velocities are expected with respect to the case of people walking in a narrow corridor. The numerical results show a strong influence of the walkway width on the mean walking velocity, especially when the footbridge is narrow and the density is low: the mean walking velocities tend to decrease on decreasing width. Conversely, for high crowd density, the mean walking velocity is not affected by the footbridge width.

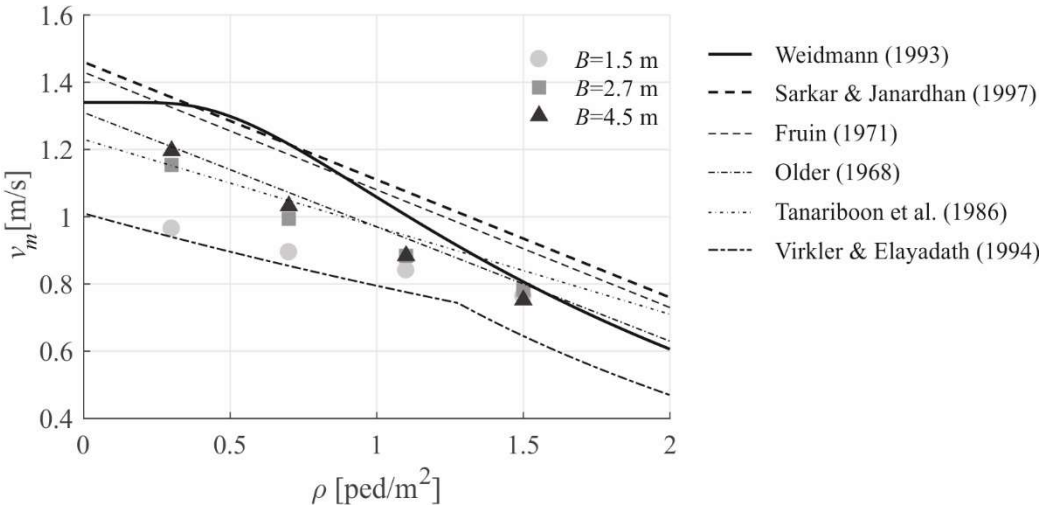

Figure 2: Velocity-density relations: comparison between numerical results and experimental data reported by the literature (after Daamen, 2004).

Instantaneous step frequencies are derived from walking velocities through Equation (10). In order to account for the reaction time needed by pedestrians to adapt their step frequency to variations of the walking velocity, the step frequency is estimated as the 5s-moving average of the instantaneous values. Step frequencies are analyzed statistically: for each crowd density and for each deck width, the pdf, the mean value and the standard deviation are derived.

Figure 3 plots the obtained numerical pdfs of the step frequencies and their Gaussian fitting, together with the model adopted in Ferrarotti and Tubino (2016). The numerical pdfs are well approximated by a Gaussian fitting, except for B = 4.5 m and $\rho \geqslant$ 1.1 ped/m^2. In these two cases, the numerical distribution appears to be asymmetric and bimodal. Unfortunately, most of the literature dealing with experimental measurements reports mean values and standard deviations of the walking velocity, without providing the corresponding pdfs. A bimodal distribution of the walking velocity has been reported by Chandra and Bharti (2013). Figure 3 also shows that simulation results cannot be reproduced assuming n_m from Equation (10) and n_{std} = 0.18 Hz, as suggested by Ferrarotti and Tubino (2016). In particular, it is evident that the

numerical distributions are shifted to the left-hand side (lower mean value) and are much narrower (lower standard deviation) with respect to the model adopted by Ferrarotti and Tubino (2016).

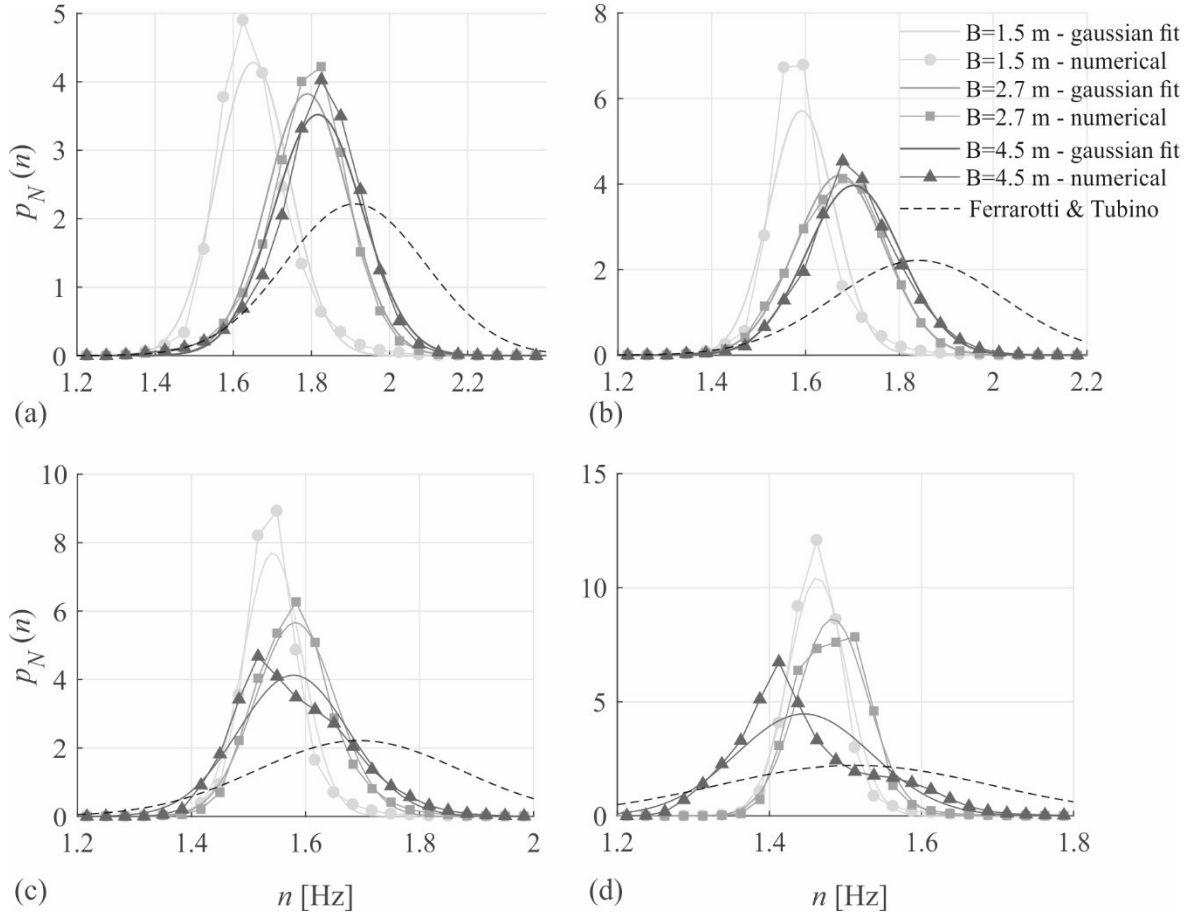

Figure 3: Numerical pdfs of the mean step frequencies and Gaussian fitting for $\rho = 0.3$ (a), $\rho = 0.7$ (b), $\rho = 1.1$ (c) and $\rho = 1.5$ ped/m^2 (d).

Figure 4 and Table 4 report the mean (Fig. 4a) and standard deviation (std) (Fig. 4b) of the step frequency obtained from Gaussian fitting for each crowd density and each footbridge width B. In line with the velocity-density trend in Figure 2, numerical mean step frequencies decrease on increasing crowd density and on increasing walkway width. For all the considered widths, numerically-obtained mean values have a trend in line with Equations (10) and (11) on increasing density. However, when the deck width is small, numerically-obtained mean step frequencies are smaller than those provided by Equations (10) and (11). Std values also show a decreasing trend for increasing crowd density, meaning that in crowded conditions pedestrians tend to walk at step frequencies closer to the mean value. It should be remarked that std values for $B = 4.5$ m and $\rho \geq 1.1$ ped/m^2 are much higher than the ones corresponding to smaller widths. However, the numerical distribution is not properly fitted by the Gaussian distribution in those cases (see Fig. 3). Figure 4b also reports some experimental std values taken from the literature, showing that the obtained numerical values are in line with experimental results. In particular, numerical results obtained for $B = 1.5$ m are in perfect accordance with experimental results reported by Butz et al. (2008), where a walking path of width $B = 1.5$ m has been considered and very low values of the standard deviation are reported. Std values obtained for larger B are higher but always in line with experimental results reported in the literature.

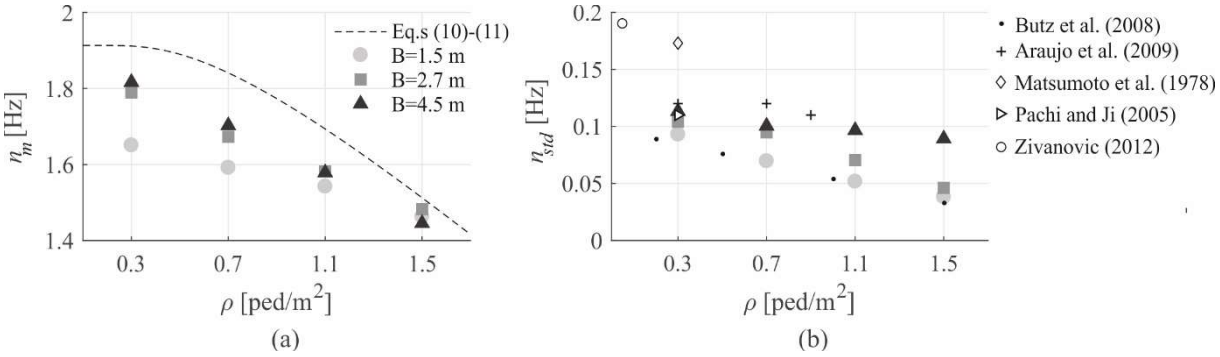

Figure 4: Numerical mean (a) and std (b) of step frequencies as functions of pedestrian density.

		ρ [ped/m^2]			
		0.3	0.7	1.1	1.5
n_m [Hz]	B = 1.5 m	1.6509	1.5920	1.5425	1.4631
	B = 2.7 m	1.7894	1.6732	1.5822	1.4831
	B = 4.5 m	1.8166	1.7027	1.5789	1.4455
n_{std} [Hz]	B = 1.5 m	0.0931	0.0697	0.0518	0.0382
	B = 2.7 m	0.1042	0.0949	0.0704	0.0462
	B = 4.5 m	0.1133	0.1005	0.0966	0.0892

Table 4: Numerical mean and std of step frequencies.

3.3 Spectral properties of pedestrian-induced loading

Pedestrian-induced forces are calculated according to Equation (5), with each contribution given by Equation (6), and the modal force is calculated as in Equation (4), assuming $\alpha_i G_i = \alpha_m G_m$ = 280 N and a time step T_s = 0.01 s. Then, for each pedestrian density and deck width, the psdf of the modal load is estimated adopting the Welch method with window length equal to 2^{12} and 50% window overlap and performing an average among the 100 simulations.

As sample cases, Figure 5 and Figure 6 plot the time history of step frequency (Fig. 5a) and force (Fig. 5b) exerted by one pedestrian, and the time history of the modal force obtained from a sample simulation (B = 2.7 m, ρ = 0.7 ped/m^2), respectively.

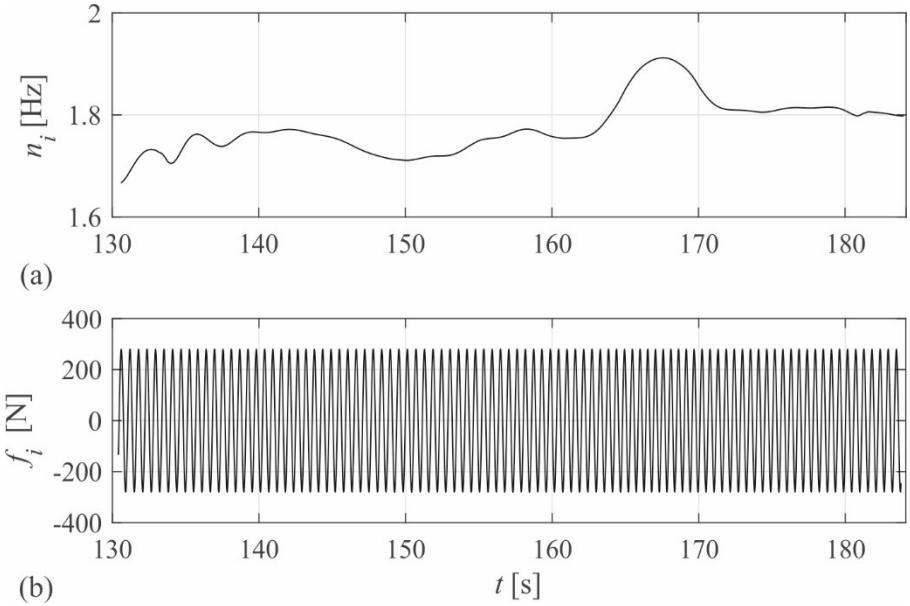

Figure 5: Time history of step frequency (a) and force (b) exerted by one pedestrian (B = 2.7 m, ρ = 0.7 ped/m^2).

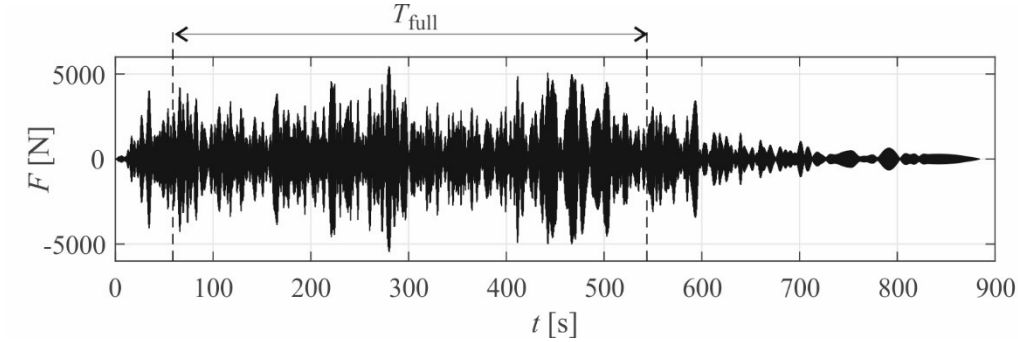

Figure 6: Time history of the modal force (B = 2.7 m, ρ = 0.7 ped/m^2).

Figure 7 plots the psdfs of the modal force obtained from numerical simulations, compared with the analytical estimates obtained from the GESM (Equation (13)). Analogously to what already observed in Figure 3 with reference to the pdf of the step frequency, it can be deduced that the harmonic content of the modal load tends to move towards lower frequencies on increasing pedestrian density. Furthermore, on increasing density, the bandwidth of the psdf of the modal load tends to decrease. The comparison with the original GESM formulation by Ferrarotti and Tubino (2016) shows that the numerically-estimated psdf is not well predicted by the GESM. In particular, three are the main discrepancies between the numerical and the analytical prediction:

- the average harmonic content of the modal loading predicted by GESM is shifted towards higher frequencies with respect to the numerical estimate;
- the bandwidth of the psdf of the modal load predicted by the GESM is larger than the numerical estimate;
- the GESM significantly underestimates the numerical psdf for low densities, while it overestimates the numerical psdf for high density.

It should be pointed out that the harmonic content of the modal loading predicted by the GESM is proportional to the pdf of the step frequency. Thus, a shift of the harmonic content in the GESM can be obtained by modifying the mean value of the step frequency. Furthermore,

the original GESM formulation, assuming a fixed standard deviation of the step frequency and a frequency-independent model for the coherence function, is not able to capture the variation of the bandwidth in the harmonic content on varying pedestrian density obtained from numerical simulations. This variation can be captured by assuming density-dependent standard deviation of the step frequency or a frequency-dependent model for the coherence function. Finally, the overestimate of the modal load provided by the GESM may be related to the adopted coherence function.

Based on these observations, a Modified GESM (M-GESM) is proposed. In the M-GESM, the interaction among pedestrians is modelled through density-dependent values of the mean and standard deviation of the step frequency, which tends to decrease on increasing density. The coherence function is instead assumed as the one originally proposed for unrestricted traffic. Thus, the psdf of the modal force provided by M-GESM is given by Equation (15), with the pdf of the step frequency being a Gaussian characterized by the density-dependent mean and standard deviation values provided in Table 4.

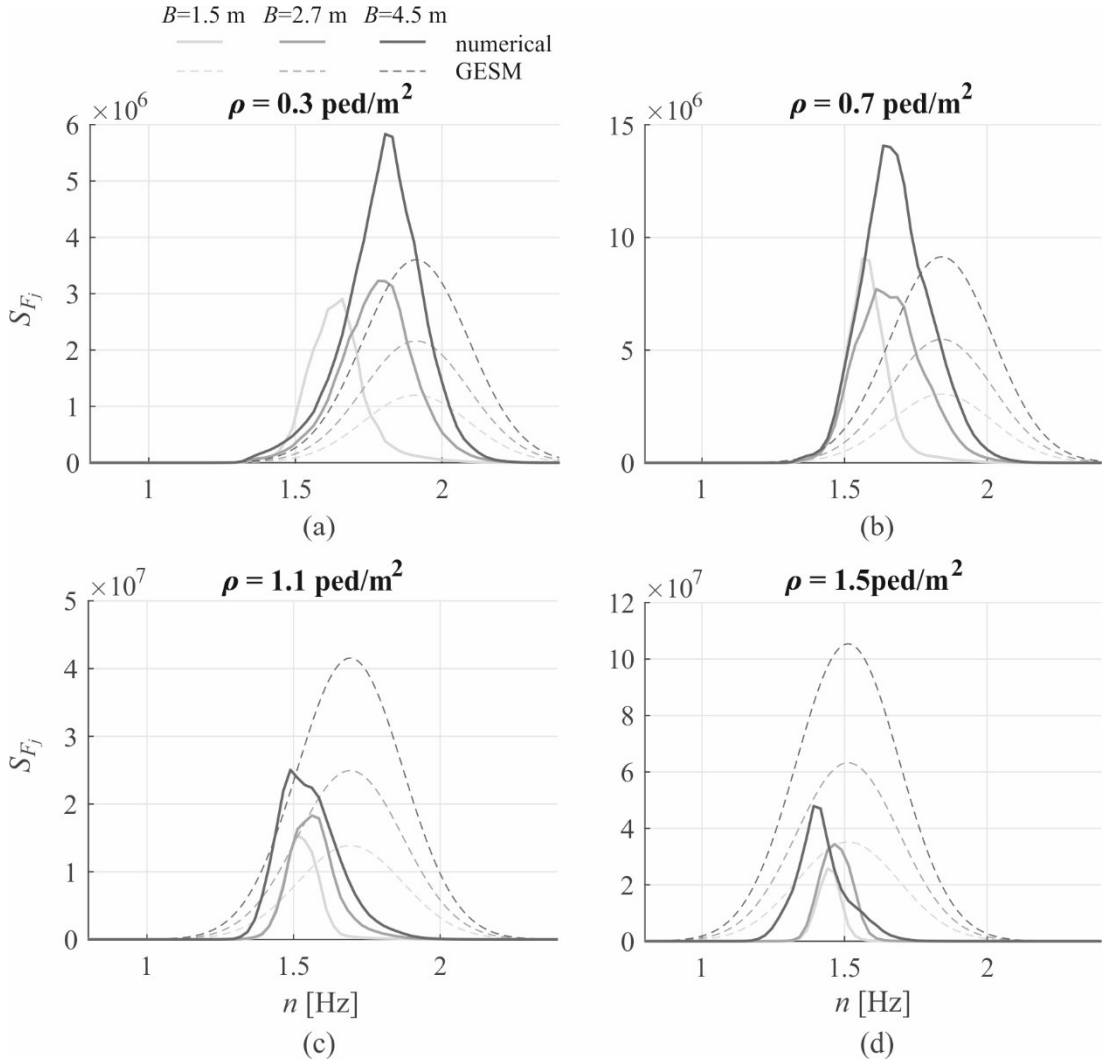

Figure 7: Comparison between psdfs of the modal force obtained from numerical simulations (solid lines) and GESM predictions for ρ = 0.3 (a), 0.7 (b), 1.1 (c) and 1.5 ped/m^2 (d).

Figure 8 plots the psdfs of the modal force obtained from numerical simulations, compared with the analytical estimates obtained from the M-GESM. The analytical solution provided by the M-GESM is now in good accordance with numerical simulations. For the cases where the numerical distributions of step frequencies are not adequately fitted by Gaussian distribution (B = 4.5 m and $\rho \geq 1.1$ ped/m^2), the M-GESM is less reliable, but it performs much better than the original formulation in Figure 7. In these cases, a better fitting could be achieved by adopting the numerical distribution of step frequencies (Figure 3) instead of the Gaussian.

This observation supports the assumption that interaction among pedestrians can be globally modelled assuming a psdf of the modal load provided by the GESM for unrestricted traffic and adopting a pdf of the step frequency coherent with simulations, i.e., taking into account the reduction of its mean and std value on increasing crowd density. It should be remarked that, in any case, the psdf of the modal load slightly deviates from the Gaussian: this deviation cannot be captured assuming a frequency-independent coherence function (Equation (12)). As a consequence, the admittance function (Equation (14)) does not depend on frequency and the spectrum of the modal load has the same shape as the one of the force per-unit-length (Equation (13)). Better agreement between the numerically-estimated psdf and the GESM proposal could be obtained adopting a frequency-dependent coherence model.

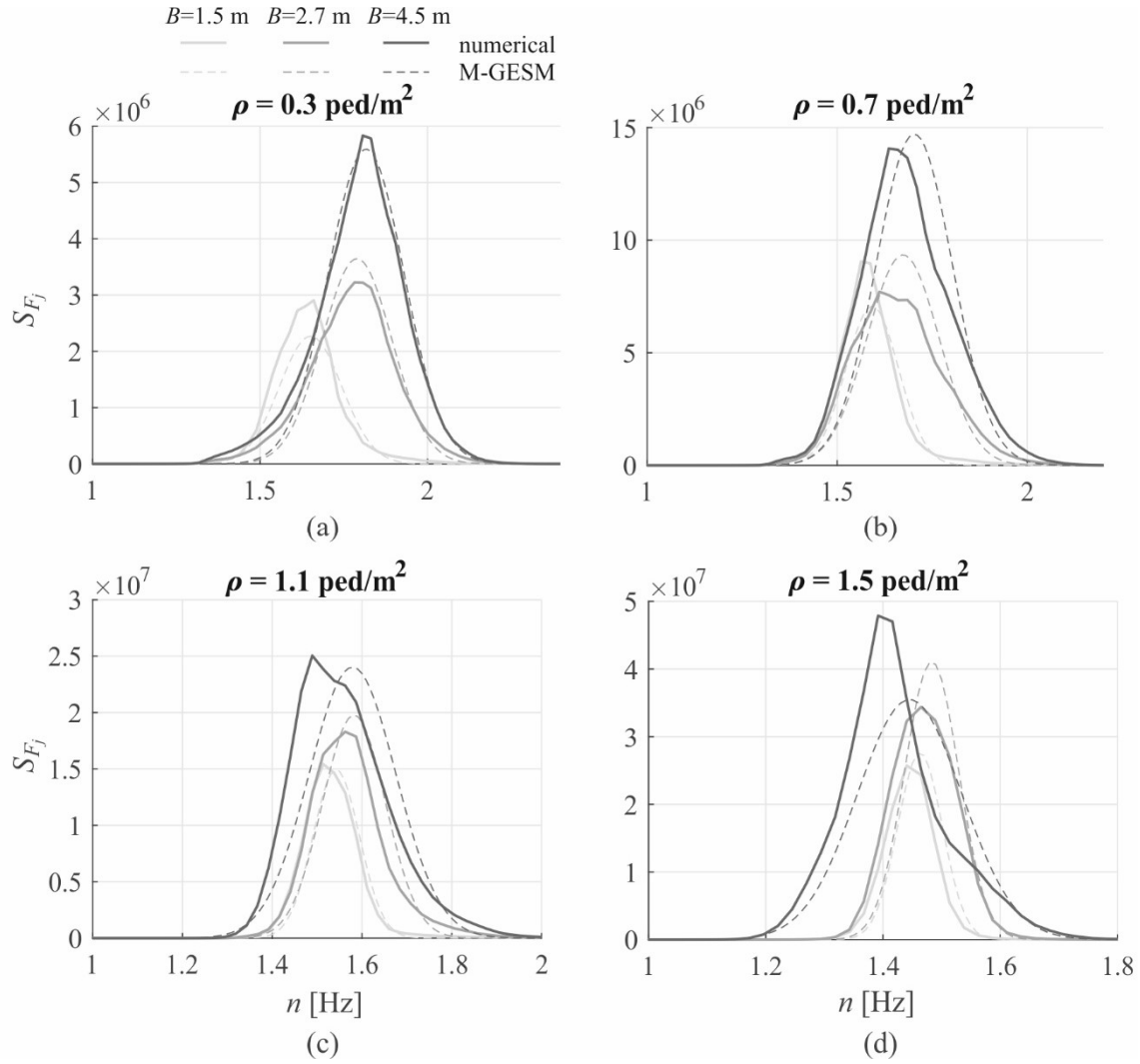

Figure 8: Comparison between psdfs of the modal force obtained from numerical simulations and M-GESM predictions for ρ = 0.3 (a), 0.7 (b), 1.1 (c) and 1.5 ped/m^2 (d).

4 NUMERICAL APPLICATIONS – FOOTBRIDGE DYNAMIC RESPONSE

In this Section, two numerical applications are considered in order to assess the capability of the simplified procedures suggested by advanced guidelines (HiVOSS) and of the M-GESM to predict maximum footbridge accelerations in line with those obtained numerically from Monte Carlo simulations of restricted pedestrian flows. Four crowd densities (ρ = 0.3, 0.7, 1.1, 1.5 ped/m^2) are considered, and the dynamic response is evaluated according to the time-domain approach, the spectral approach based on the M-GESM discussed in Section 3.3 and the simplified procedures suggested by HiVOSS.

The first example is a real footbridge that was experimentally tested, characterized by a natural frequency higher than typical mean step frequencies in unrestricted traffic conditions. The second application concerns an ideal footbridge with a natural frequency smaller than typical pedestrian mean step frequency in unrestricted conditions.

4.1 Example 1: a real footbridge

The De Gasperi Footbridge (Tubino et al., 2016) is characterized by a width B = 2.7 m, a length L = 60 m, and the following dynamic properties: n_1 = 2.17 Hz, M_1= 51000 kg, ξ_1 = 0.005. The first mode shape can be approximated by a sinusoidal function $\varphi_1(x) = \sin(\pi x/L)$.

Figure 9 compares the maximum dynamic response obtained from time-domain numerical simulations with the one obtained through the M-GESM (Equation (20)) and with the prediction estimated adopting the two simplified procedures suggested by HiVOSS (Equations (23) and (24)). Both numerical simulations and M-GESM provide a decreasing trend of maximum dynamic response on increasing pedestrian density. This is due to the significant effect of pedestrian interaction, causing a decrease of the mean step frequency and of its standard deviation on increasing pedestrian density. Thus, the intensity of pedestrian-induced loading increases, but its harmonic content progressively changes. The effect of this change on the dynamic response depends on the dynamic properties of the considered structure. For the numerical example considered here, the harmonic contribution of the loading tends to move away from the natural frequency of the structure, causing a decrease in the dynamic response.

In contrast with numerical simulation results, HiVOSS SDOF method provides an increasing maximum dynamic response of the footbridge on increasing pedestrian density. Furthermore, accelerations are greatly overestimated. HiVOSS response spectra method provides lower accelerations with respect to the SDOF method, but it is still extremely over-conservative for this case study, especially for high pedestrian density.

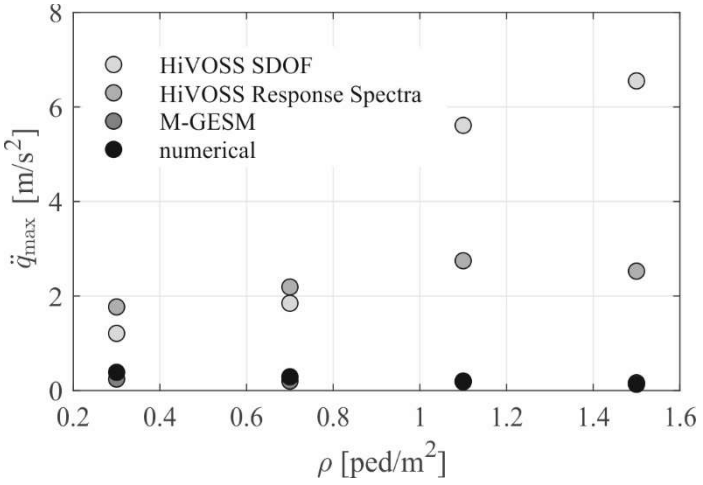

Figure 9: De Gasperi Footbridge: maximum value of mid-span acceleration.

In order to better understand the cause of the difference between the numerical prediction and the M-GESM, Figure 10 plots the psdf of the mid-span acceleration: results obtained from the numerical solution of the equation of motion (dotted lines) are compared with the analytical estimate based on the M-GESM, provided by Equation (16) (solid lines). For low pedestrian density (ρ = 0.3, 0.7 ped/m^2), the resonant contribution to the structural response is not negligible, and it is underestimated by the M-GESM due to the approximation of the psdf of the loading model (see Figure 8). For high pedestrian density (ρ = 1.1, 1.5 ped/m^2), the resonant contribution to the dynamic structural response is negligible, and the M-GESM results are in better accordance with numerical solutions.

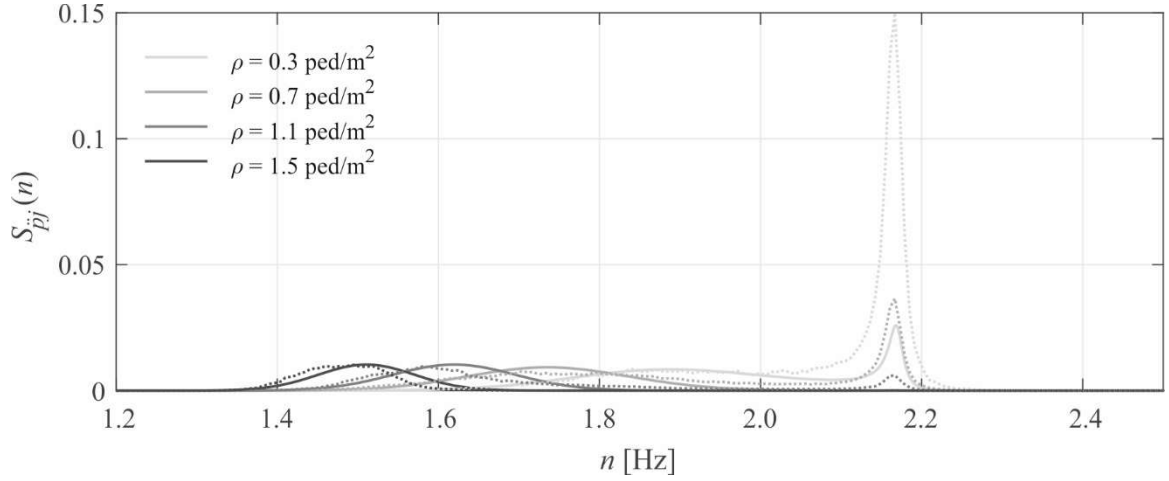

Figure 10: De Gasperi Footbridge: psdf of the mid-span acceleration.

4.2 Example 2: ideal footbridge

The ideal footbridge here considered is the same already studied in Ferrarotti and Tubino (2016). It has the same geometric properties as the De Gasperi Footbridge (B = 2.7 m, L = 60 m), but different dynamic properties: n_1 = 1.65 Hz, M_1= 151000 kg, ξ_1 = 0.005. The first mode shape can be approximated by a sinusoidal function $\varphi_1(x) = \sin(\pi x/L)$.

Analogously to Figure 9, Figure 11 compares the maximum dynamic response obtained from numerical simulations with the one obtained through the M-GESM (Equation (19)) and with the prediction estimated adopting the two simplified procedures suggested by HiVOSS (Eqs. (23) and (24)). Also in this case, the trend of the maximum dynamic response on increasing pedestrian density predicted by the M-GESM is in accordance with numerical simulations. Differently from Figure 9, the trend is not monotonically decreasing: the dynamic response is maximum for the pedestrian density ρ =1.1 ped/m^2: this is due to the fact that, for this value of pedestrian density, the mean step frequency is very close to the natural frequency of the footbridge (Table 4). The M-GESM tends to overestimate the maximum acceleration obtained from numerical simulations, especially for ρ > 0.3 ped/m^2.

Analogously to Example 1, HiVOSS SDOF method provides an increasing maximum dynamic response on increasing pedestrian density and it greatly overestimates maximum accelerations for high pedestrian density. HiVOSS response spectra method provides a trend of the maximum acceleration on increasing pedestrian density in accordance with numerical

simulations, but for intermediate values of pedestrian density it tends to underestimate the maximum dynamic response of the footbridge.

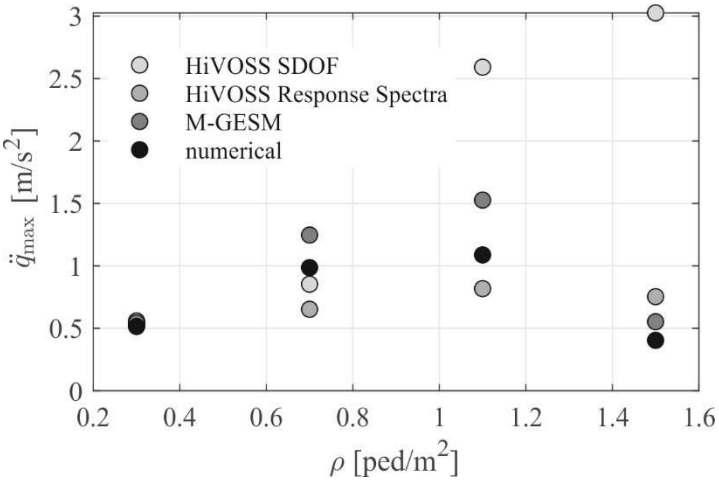

Figure 11: Ideal Footbridge: maximum value of mid-span acceleration.

Figure 12 plots the psdf of the mid-span acceleration. Results obtained from the numerical simulations (dotted lines) are compared with the analytical estimate based on the M-GESM, provided by Equation (16) (solid lines). In this case, for any value of pedestrian density, the dynamic response is mainly resonant and its psdf is overestimated by the M-GESM. This is due to the overestimate of the psdf of the modal loading provided by the M-GESM for frequencies around 1.65 Hz (Fig. 8).

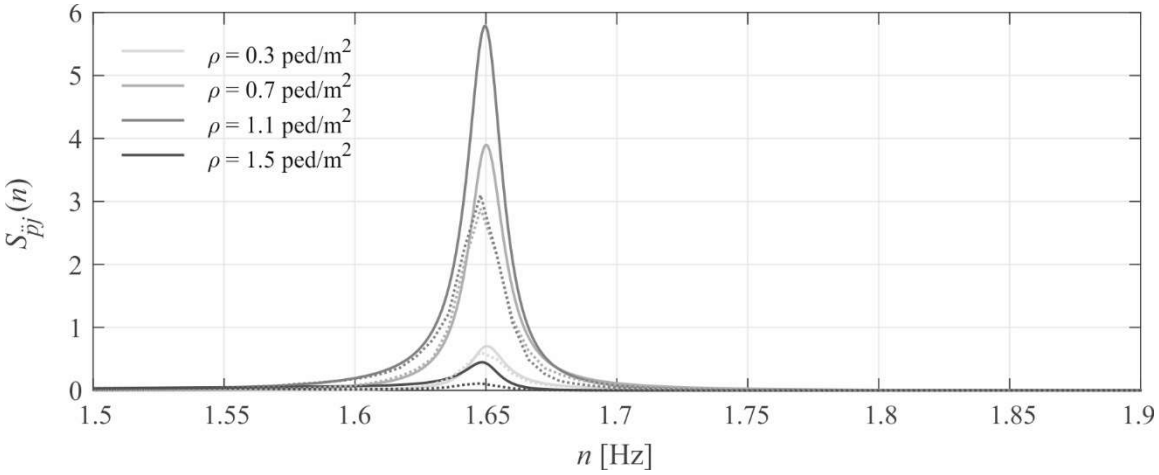

Figure 12: Ideal Footbridge: psdf of the mid-span acceleration.

5 CONCLUSIONS AND PROSPECTS

This paper studied the pedestrian-induced force and the dynamic response of footbridges in restricted pedestrian traffic conditions, based on numerical simulations of the crowd dynamics, for densities ranging from 0.3 ped/m^2 to 1.5 ped/m^2 and different deck widths. Original results have been obtained regarding the probability distribution of the step frequency and the spectral

characterization of the loading. Furthermore, the reliability of available procedures for the vibration serviceability assessment of footbridges has been analyzed.

The probabilistic analysis of the step frequency has revealed that, in accordance with fundamental laws from the literature, the mean step frequency tends to decrease on increasing crowd density. Furthermore, also the standard deviation of the step frequency tends to decrease in crowded conditions. Numerical results have also highlighted that the probability distribution of the step frequency is affected by the deck width. For low crowd density, the mean walking frequency tends to decrease on decreasing footbridge width. This effect tends to vanish for high crowd density.

The analysis of the psdf of the modal force has shown that it is proportional to the probability density function of the step frequency. The Generalized Equivalent Spectral Model proposed by Ferrarotti and Tubino (2016) tends to significantly overestimate the psdf of the modal load for high pedestrian density and it does not allow to predict in a reliable way the harmonic content of the modal loading. Thus, a modified formulation for the Generalized Equivalent Spectral Model has been introduced, which allows to obtain psdf of the modal load in good accordance with numerical simulations. In particular, in the Modified Generalized Equivalent Spectral Model, the coherence model proposed by Ferrarotti and Tubino (2016) for unrestricted pedestrian traffic is considered, and density-dependent values of the mean and standard deviation of the step frequency are assumed.

The numerical applications have shown that the variation of the harmonic content of the loading due to pedestrian interaction can have significant effects on the footbridge dynamic response. The SDOF method proposed by HiVOSS, analogous to the one suggested by SETRA, is not able to capture the trend of the dynamic response with increasing density and provides very conservative estimates of the maximum footbridge acceleration, especially for high pedestrian density. The response spectra method by HiVOSS provides results closer to the numerical estimates, but not always conservative. The M-GESM allows to capture the trend of the dynamic response with increasing pedestrian density. The accordance between the dynamic response estimated numerically and through the M-GESM strongly depends on the footbridge natural frequency. In general, the higher the deviation from the Gaussian of the psdf of the modal load, the higher the discrepancy between numerical and M-GESM estimated results.

The obtained results have highlighted the importance of a reliable characterization of the shape of the psdf of the modal load. This could be achieved through a refined model for the coherence of the equivalent loading, e.g., a frequency-dependent coherence model could allow to obtain a better accordance with numerical results. With this aim, a strategy to directly characterize the power spectral density and the coherence functions of the equivalent distributed loading is under investigation. Finally, it should be underlined that the availability of experimental measurements of step frequency and pedestrian-induced loading in different traffic conditions (from sparse to dense) is crucial for a thorough validation of the proposed model.

ACKNOWLEDGEMENTS

F. Venuti wishes to thank Oasys Software Ltd for having provided free license of the software MassMotion. In particular, Zeena Farouk and Lachlan Miles are greatly acknowledged for their support and for having supplied technical documentation and scientific references about MassMotion working principles.

REFERENCES

Araújo, M.C., Brito, H.M.B.F. & Pimentel, R.L. (2009). Experimental evaluation of synchronisation in footbridges due to crowd density. *Structural Engineering International,* 19(3), 298–303.

Arup (2017). *MassMotion v9.5 User manual*. Oasys Software Ltd.

Arup (2020a). *QA Testing of MassMotion 10.5*, Version 1, 13 August 2020.

Arup (2020b). *Verification testing of MassMotion 10.5 for evacuation modelling*, Version 1, 13 August 2020.

Bassoli, E., Van Nimmen, K., Vincenzi, L. & Van den Broeck, P. (2018). A spectral load model for pedestrian excutation including vertical human-structure interaction. *Engineering Structures,* 156, 537–547.

Brownjohn, J.M.W., Pavic, A. & Omentzetter, P.A. (2004). Spectral density approach for modelling continuous vertical forces on pedestrian structures due to walking. *Canadian Journal of Civil Engineering,* 31(1), 65-77.

Butz, C., Feldmann, M., Heinemeyer, C., Sedlacek, G., Chabrolin, B., Lemaire, A., et al. (2008). *Advanced load models for synchronous pedestrian excitation and optimised design guidelines for steel footbridges SYNPEX.* (Report No. RFS-CR 03019). Research Fund for Coal and Steel.

Caprani, C.C., Keogh, J., Archbold, P. & Fanning, P. (2012). Enhancement for the vertical response of footbridges subjected to stochastic crowd loading. *Computers and Structures,* 102-103, 87–96.

Caprani, C. & Ahmadi, E. (2016). Formulation of human-structure interaction system models for vertical vibration. *Journal of Sound and Vibration,* 377, 347-367.

Carroll, S.P., Owen, J.S. & Hussein, M.F.M. (2012). Modelling crowd–bridge dynamic interaction with a discretely defined crowd. *Journal of Sound and Vibration,* 331, 2685–2709.

Challenger, R., Clegg, C.W. & Robinson, M.A. (2009). *Understanding Crowd Behaviours. Supporting evidence*, UK Cabinet Office.

Chandra, S. & Bharti, A.K. (2013). Speed distribution curves for pedestrians during walking and crossing. *Procedia – Social and Behavioral Sciences,* 104, 660-667.

Daamen, W. (2004). *Modelling passengers flow in public transport facilities*. [Doctoral dissertation, TU Delft], TU Delft Repository https://repository.tudelft.nl/islandora/object/uuid%3Ae65fb66c-1e55-4e63-8c49-5199d40f60e1 .

Dang, H.V. & Zivanovic, S. (2015). Experimental characterisation of walking locomotion on rigid level surfaces using motion capture system. *Engineering Structures,* 91, 141-154.

Davenport, A.G. (1964). Note on the distribution of the largest value of a random function with application to the gust loading. *Proceedings of the Institution of Civil Engineers,* 28(2), 187–196.

Feldmann, M. (ed). (2008). *HiVOSS—Human-induced vibrations of steel structures*. Office for Official Publications of the European Communities.

Ferrarotti, A. & Tubino, F. (2016). Generalized Equivalent Spectral Model for serviceability analysis of footbridges. *Journal of Bridge Engineering ASCE,* 21(12), Article 04016091.

Fruin, J. (1971). *Pedestrian Planning and Design*. Metropolitan Association of Urban Designers and Environmental Planners.

Fujino, Y. & Siringoringo, D.M. (2016). A Conceptual Review of Pedestrian-Induced Lateral Vibration and Crowd Synchronization Problem on Footbridges, *Journal of Bridge Engineering ASCE*, 21(8), Article C4015001.

Gao, Y-A., Yang, Q-S. & Qin, J-W. (2017). Bipedal Crowd–Structure Interaction Including Social Force Effects. *International Journal of Structural Stability and Dynamics,* 17(7), Article 1750079.

He, W. & Xie, W. (2018). Characterization of stationary and walking people on vertical dynamic properties of a lively lightweight bridge, *Structural Control and Health Monitoring*, 25(3), Article e2123.

Helbing, D. & Molnar, P. (1995). Social force model for pedestrian dynamics. *Physical Review,* 51(5), 4282–4286.

Lathi, B.P. (1998). *Modern digital and analog communication systems*. Third Edition. Oxford University Press, New York.

Macdonald, J. (2009). Lateral excitation of bridges by balancing pedestrians. *Proceedings of the Royal Society A – Mathematical, Physical and Engineering Sciences,* 465, 1055–1073.

Matsumoto, Y., Nishioka, T., Shiojiri, H. & Matsuzaki, K. (1978). Dynamic design of footbridges. *IABSE Proceedings*, P-17/78, 1–15.

Pachi, A. & Ji, T. (2005). Frequency and velocity of people walking. *The Structural Engineer,* 83(3), 36-40.

Piccardo, G. & Tubino, F. (2012). Equivalent spectral model and maximum dynamic response for the serviceability analysis of footbridges. *Engineering Structures,* 40, 445-456.

Pimentel, R.L., Araújo Jr., M.C., Brito, H.M.B.F. & Vital de Brito, J.L. (2013). Synchronization among pedestrians in footbridges due to crowd density. *Journal of Bridge Engineering, ASCE*, 18(5), 400-408.

Racic, V. & Brownjohn, J.M.W. (2011). Stochastic model of near-periodic vertical loads due to humans walking. *Advanced Engineering Informatics,* 25, 259-275.

Rivers, E., Jaynes, C., Kimball, A., Morrow, E. (2014). Using case study data to validate 3D agent-based pedestrian simulation tool for egress modeling. *Transportation Research Procedia,* 2, 123-131.

Sahnaci, C. & Kasperski, M. (2005). Random loads induced by walking. In C. Soize & G.I. Schueller (Ed.), *Proceedings of the 6th European Conference on Structural Dynamics EURODYN 2005*, (pp. 441-446). Millpress.

Sahnaci, C. & Kasperski, M. (2011). Simulation of random pedestrian flow. In G. Roeck (Ed.), *Proceedings of the 8th International Conference on Structural Dynamics EURODYN 2011*. (pp. 1040-1047). Katholieke Universiteit Leuven.

Shahabpoor, E., Pavic, A. & Racic, V. (2016). Interaction between Walking Humans and Structures in Vertical Direction: A Literature Review. *Shock and Vibration*, Article 3430285.

SETRA (2006). *Footbridges – Assessment of vibrational behaviour of footbridges under pedestrian loading.* Technical Department for Transport, Roads and Bridges Engineering and Road Safety. Ministry of Transport and Infrastructure.

Tubino, F., Carassale, L. & Piccardo, G. (2016). Human-induced vibrations on two lively footbridges in Milan. *Journal of Bridge Engineering ASCE*, 21(8), Article C4015002.

Tubino, F. & Piccardo, G. (2016). Serviceability assessment of footbridges in unrestricted pedestrian traffic condition. *Structure and Infrastructure Engineering,* 12(12), 1652-1662.

Tubino, F. (2018). Probabilistic assessment of the dynamic interaction between multiple pedestrians and vertical vibrations of footbridges. *Journal of Sound and Vibration,* 417, 80-96.

Van Nimmen, K., Lombaert, G., De Roeck, G., & Van den Broeck, P. (2014). Vibration serviceability of footbridges: Evaluation of the current codes of practice. *Engineering Structures,* 59, 448–461.

Van Nimmen, K., Lombaert, G., De Roeck, G. &. Van den Broeck, P. (2017). The impact of vertical human-structure interaction on the response of footbridges to pedestrian excitation. *Journal of Sound and Vibration,* 402, 104–121.

Van Nimmen, K., Van den Broeck, P., Lombaert, G. & Tubino, F. (2020). Pedestrian-induced vibrations of footbridges: An extended spectral approach. *Journal of Bridge Engineering,* 25(8), Article 04020058.

Venuti, F. & Bruno, L. (2007). An interpretative model of the pedestrian fundamental relation. *Comptes Rendus Mecanique,* 335(4), 194-200.

Venuti, F., Racic, V. & Corbetta, A. (2016). Modelling framework for dynamic interaction between multiple pedestrians and vertical vibrations of footbridges. *Journal of Sound and Vibration,* 379, 245-263.

Venuti, F. & Reggio, A. (2018). Mitigation of human-induced vertical vibrations of footbridges through crowd flow control. *Structural Control and Health Monitoring*, 25, Article e2266.

Živanović, S., Pavic, A. & Reynolds, P. (2005). Vibration serviceability of footbridges under human-induced excitation: a literature review. *Journal of Sound and Vibration,* 279(1-2), 1–74.

Živanović, S., Pavic, A. & Reynolds, P. (2007). Probability-based prediction of multi-mode vibration response to walking excitation. *Engineering Structures*, 29(6), 942–954.

Živanović, S., Pavic, A. & Ingolfsson, E.T. (2010). Modelling spatially unrestricted pedestrian traffic on footbridges. *Journal of Structural Engineering,* 136(10), 1296–1308.